Phase noise mitigation by realistic optical parametric oscillator

MICHELE N. NOTARNICOLA[1], MARCO G. GENONI,[1,2] SIMONE CIALDI,[1,2], MATTEO G. A. PARIS,[1,2] AND STEFANO OLIVARES[1,2,*]

[1] *Dipartimento di Fisica "Aldo Pontremoli," Università degli Studi di Milano, I-20133 Milano, Italia*
[2] *Istituto Nazionale di Fisica Nucleare, Sezione di Milano, I-20133 Milano, Italia*
[*] *stefano.olivares@fisica.unimi.it*

Abstract: We address the exploitation of an optical parametric oscillator (OPO) in the task of mitigating, at least partially, phase noise produced by phase diffusion. In particular, we analyze two scenarios where phase diffusion is typically present. The first one is the estimation of the phase of an optical field, while the second involves a quantum communication protocol based on phase shift keying. In both cases, we prove that an OPO may lead to a partial or full compensation of the noise.

1. Introduction

The phase of an optical field is a fundamental degree of freedom for several applications in quantum sensing and quantum communication. Quantum interferometry is exploited in high-precision measurements to detect fine perturbations through phase shifts [1–3] and continuous-variable communication protocols are often based on *phase shift keying* (PSK) [4–6]. However, the optical phase cannot be described as an observable in a strict sense [7–10] and this result makes it challenging to provide a detailed description of all the strategies involving the phase.

In practical contexts the phase of a field is often affected by phase noise especially due to phase diffusion. Indeed, the presence of phase diffusion may lead to a partial or complete loss of all the advantages of quantum measurements. In the quantum optics scenario, phase diffusion efficiently describes the noisy propagation of quantum light through optical fibers [11], and its effect has been thoroughly investigated on phase estimation and quantum communication protocols [12–19]. More generally, its detrimental effects have been also investigated for different physical platforms, such as Bose-Einstein condensates [20, 21] and Bose-Josephson junctions [22].

Focussing our attention on quantum optical systems, one of the possible resources to counteract phase noise is provided by a phase-sensitive amplifier, such as a *optical parametric oscillator* (OPO). More precisely, an OPO is not expected to be useful to improve measurements, i.e. to build receivers, because the induced phase shift would lead to a modification of the phase outcome. On the contrary, an OPO may be very effective at the preparation stage of a communication scheme, in order to improve the properties of the probe state if affected by phase noise.

In this work, we address the possibility of using an OPO to compensate, at least partially, the detriments of phase noise. Hints that squeezing could help in this scenario have already been shown in [23, 24]. Here we discuss in more detail a realistic experimental implementation of a squeezing operation via an OPO, taking into account the most relevant experimental details. Moreover, we consider two different scenarios in which an optical phase is exploited. The first one is a pure *quantum optical* context and regards the measurement of the phase of a quantum state of radiation. On the contrary, the second case consists of a *quantum communication scheme* where information is encoded on a phase shift. In both cases we consider single mode radiation prepared in a coherent state $|\alpha\rangle$, $\alpha \in \mathbb{R}_+$ undergoing phase diffusion. Just after dephasing, we introduce an OPO and discuss if its exploitation may lead to noise mitigation.

The paper is structured as follows. First of all, in sec. 2 we give a brief recap of quantum estimation theory, which will be exploited for the second scenario in exam. Then, in sec. 3 we present a theoretical model for the OPO, described in the Schrödinger picture, allowing to work directly at the level of quantum states. Bearing that in mind, we apply it to the two scenarios in exam. In sec. 4 we address the measurement of an optical phase and state in which conditions the OPO is able to counteract phase noise while sec. 5 is dedicated to describe the communication protocol and to find out the optimal measurement to detect the value of the encoded phase shift with the highest possible precision. We close our investigation drawing some concluding remarks in sec. 6.

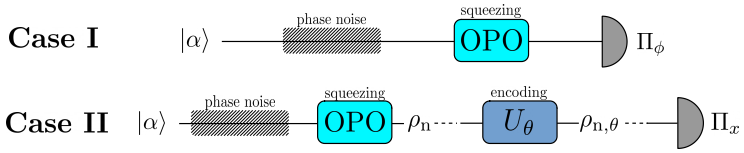

Fig. 1. Schematic diagram of the two scenarios discussed in this paper.

2. Elements of quantum estimation theory

The estimation of a parameter is a frequent task in quantum mechanics, since several physical quantities cannot be directly measured. Here we present the basic features of the theory behind it [25, 26]. We consider a family of quantum states labelled by a parameter λ, $\{\rho_\lambda\}_\lambda$, usually called *statistical model*. Usually, we perform a generalized measurement described by a positive operator-valued measure (POVM) $\{\Pi_x\}$, obtaining a statistical sample of M outcomes $\mathbf{x} = \{x_1, ..., x_M\}$. This sample is processed by means of a map $\hat{\lambda}(\mathbf{x})$, called an *estimator*, to infer the value of the parameter λ. The task is to find the optimal POVM that allows to estimate the value of λ with the lowest possible uncertainty, i.e., the maximum precision. The conditional probability of the outcome x given λ is

$$p(x|\lambda) = \mathrm{Tr}[\rho_\lambda \Pi_x]. \tag{1}$$

If the estimator is unbiased, there exists a lower bound to its variance, depending on the *Fisher information* (FI) of the distribution $p(x|\lambda)$

$$F(\lambda) = \int dx \frac{\left[\partial_\lambda p(x|\lambda)\right]^2}{p(x|\lambda)}. \tag{2}$$

The bound is the so called *Cramér-Rao bound* and reads

$$\mathrm{Var}[\hat{\lambda}] \geq \frac{1}{MF(\lambda)}, \tag{3}$$

where we introduced the variance $\mathrm{Var}[\hat{\lambda}] = \mathrm{E}[\hat{\lambda}^2] - \mathrm{E}[\hat{\lambda}]$ with

$$\mathrm{E}[\hat{\lambda}^k] = \int dx\, p(x|\lambda)\, x^k, \quad k \in \mathbb{N}. \tag{4}$$

However, a more strict bound, independent of the particular measurement performed, may be obtained [27–30]. We define the Symmetric Logarithmic Derivative (SLD) L_λ by the Ljapunov equation $2\partial_\lambda \rho_\lambda = L_\lambda \rho_\lambda + \rho_\lambda L_\lambda$ and the *Quantum Fisher Information* (QFI) as [26]

$$H(\lambda) = \mathrm{Tr}[\rho_\lambda L_\lambda^2]. \tag{5}$$

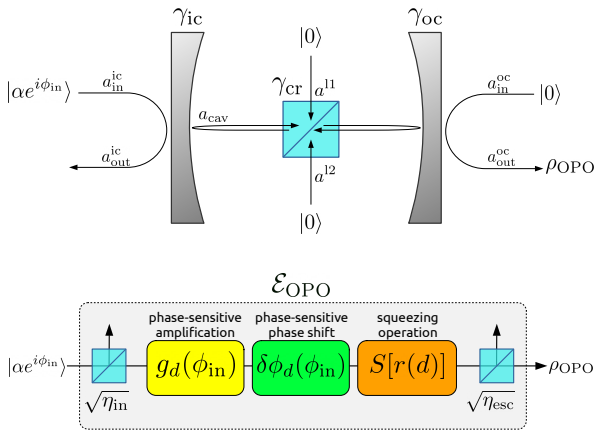

Fig. 2. Top: schematic diagram of an OPO in the input-output description with a coherent state $|\alpha e^{i\phi_{\rm in}}\rangle$ entering the input coupler. Bottom: Block scheme. The dynamics of the OPO can be described as the subsequent application of phase-sensitive amplification $g_d(\phi_{\rm in})$, phase-sensitive phase shift $\delta\phi_d(\phi_{\rm in})$ and squeezing $S[r(d)]$.

The QFI leads to the *Quantum Cramér-Rao bound*

$$\mathrm{Var}[\hat{\lambda}] \geq \frac{1}{MH(\lambda)}. \tag{6}$$

In assessing a quantum estimation scheme, both the QFI and the FI are important tools. The QFI identifies the ultimate limits on precision allowed by quantum mechanics, independent of the measurement, while the FI fixes the minimum possible uncertainty given a particular measurement strategy, namely, a POVM. In this present work we will address a subclass of possible measurements, that is homodyne measurements, and determine their performance by comparing the QFI and FI.

3. A block-diagram model for the OPO

A traditional description of the OPO is obtained by exploiting the input-output formalism [31]. As depicted in the top panel of Fig. 2, the dynamics of the OPO is characterized by the input and output modes $a^{\rm ic/oc}_{\rm in/out}$ associated with the input and output coupler, the input modes associated with the crystal losses $a^{l1/l2}$ and the coherent evolution of the cavity mode $a_{\rm cav}$ generated by the squeezing Hamiltonian $H_s = i\frac{1}{2}g(a^{\dagger 2}_{\rm cav} - a^2_{\rm cav})$, where we have assumed to fix the laser pump in order to amplify the quadrature $q = (a_{\rm cav} + a^\dagger_{\rm cav})/\sqrt{2}$ of the field inside the cavity. The input-output operators satisfy the canonical commutation relations (CCR) $[a^{\rm ic/oc}_{\rm in/out}, a^{\rm ic/oc\dagger}_{\rm in/out}] = [a^{l1/l2}, a^{l1/l2\dagger}] = 1$, while the cavity mode evolves such that $[a_{\rm cav}(t), a^\dagger_{\rm cav}(t')] = \delta(t-t')$ [31]. We now introduce the parameters $\eta_{\rm in}$ and $\eta_{\rm esc}$ and the squeezing parameter d. The input and output parameters depend on the loss rates at both the input coupler ($\gamma_{\rm ic}$) and the output coupler ($\gamma_{\rm oc}$) and the rate of internal losses of the crystal ($\gamma_{\rm cr}$), see Fig. 2. We have

$$\eta_{\rm in} = \gamma_{\rm ic}/\gamma, \quad \eta_{\rm esc} = \gamma_{\rm oc}/\gamma, \tag{7}$$

where $\gamma = \gamma_{\rm ic} + \gamma_{\rm oc} + 2\gamma_{\rm cr}$. The squeezing parameter d is proportional to the coupling of the squeezing Hamiltonian and reads $d = g/\gamma$ and the stability condition of the OPO imposes $d < 1$ [31].

By considering a roundtrip of the cavity of duration τ, defining $\tilde{a}_{\rm cav} = \sqrt{\tau} a_{\rm cav}$ and in the presence of high reflectivity mirrors, the Langevin equation for the cavity mode and its boundary condition read [31]

$$\frac{d\tilde{a}_{\rm cav}}{dt} = g\tilde{a}^{\dagger}_{\rm cav}(t) - \gamma\tilde{a}_{\rm cav}(t) + \sqrt{2\gamma_{\rm ic}}\; a^{\rm ic}_{\rm in} + \sqrt{2\gamma_{\rm oc}}\; a^{\rm oc}_{\rm in} + \sqrt{2\gamma_{\rm cr}}(a^{\rm l1} + a^{\rm l2}), \tag{8a}$$

$$a^{\rm ic/oc}_{\rm out} = -a^{\rm ic/oc}_{\rm in} + \sqrt{2\gamma_{\rm ic/oc}}\;\tilde{a}_{\rm cav}. \tag{8b}$$

Considering the device in the stationary regime, Eqs. (8) can be exploited to express the output mode in function of the input ones as

$$a^{\rm oc}_{\rm out} = d\;(a^{\rm oc\dagger}_{\rm out} + a^{\rm oc\dagger}_{\rm in}) + (\eta_{\rm esc} - \eta_{\rm in} - 2\eta_{\rm cr})a^{\rm oc}_{\rm in} + + 2\sqrt{\eta_{\rm in}\eta_{\rm esc}}a^{\rm ic}_{\rm in} + 2\sqrt{\eta_{\rm cr}\eta_{\rm esc}}(a^{\rm l1} + a^{\rm l2}), \tag{9}$$

with $\eta_{\rm cr} = \gamma_{\rm cr}/\gamma$. The last equation is not in closed form, therefore it is convenient to pass to quadratures

$$q_{\rm out} = \frac{a^{\rm oc}_{\rm out} + a^{\rm oc\dagger}_{\rm out}}{\sqrt{2}}, \quad p_{\rm out} = \frac{a^{\rm oc}_{\rm out} - a^{\rm oc\dagger}_{\rm out}}{\sqrt{2}\,i}. \tag{10}$$

For an initial coherent state at the input coupler $|\alpha e^{i\phi_{\rm in}}\rangle$, $\alpha \in \mathbb{R}_+$, and the vacuum in all other ports, the final state at the output coupler $\rho_{\rm OPO}$ is such that

$$\big\{\langle q_{\rm out}\rangle, \langle p_{\rm out}\rangle\big\} = \sqrt{2}\big\{\tilde{\alpha}_q \cos\phi_{\rm in}, \tilde{\alpha}_p \sin\phi_{\rm in}\big\}, \tag{11a}$$

$${\rm Var}[q_{\rm out}] = \frac{1}{2}\left[1 + \eta_{\rm esc}\frac{4d}{(1-d)^2}\right] \equiv \Sigma^2_q\,, \tag{11b}$$

$${\rm Var}[p_{\rm out}] = \frac{1}{2}\left[1 - \eta_{\rm esc}\frac{4d}{(1+d)^2}\right] \equiv \Sigma^2_p\,, \tag{11c}$$

with

$$\tilde{\alpha}_q = 2\frac{\sqrt{\eta_{\rm in}\eta_{\rm esc}}\;\alpha}{1-d}, \quad \tilde{\alpha}_p = 2\frac{\sqrt{\eta_{\rm in}\eta_{\rm esc}}\;\alpha}{1+d}. \tag{12}$$

In Eq. (11c) we clearly have $\Sigma^2_p < 1/2$, showing squeezing in the $p_{\rm out}$ quadrature. Moreover, two other effects induced by the OPO are a phase-sensitive amplification and a phase-sensitive phase shift. By computing expectation values on Eq. (9) with the same input states, we get

$$\langle a^{\rm oc}_{\rm out}\rangle = 2\sqrt{\eta_{\rm in}\eta_{\rm esc}}\;\alpha_{\rm out}\; e^{i\phi_{\rm out}}, \tag{13}$$

where

$$\alpha_{\rm out} = \frac{\alpha\sqrt{1 + 2d\cos(2\phi_{\rm in}) + d^2}}{1-d^2}, \tag{14a}$$

$$\tan\phi_{\rm out} = \frac{1+d}{1-d}\;\tan\phi_{\rm in}. \tag{14b}$$

An equivalent description of the OPO may be obtained working in the Schrödinger picture, through the block scheme sketched in the bottom panel of Fig. 2. We consider a single mode of radiation a entering the OPO, $[a, a^{\dagger}] = 1$. Then the block scheme consists of the

sequential application of unitary operations associated with all the transformations produced by the OPO, that is beam splitters of trasmissivity $\eta_{\rm in/esc}$ for the input and output couplers, respectively, phase-sensitive amplification $g_d(\phi_{\rm in})$, phase-sensitive phase shift $\delta\phi_d(\phi_{\rm in})$ and squeezing $S[r(d)] = \exp\{\frac{1}{2}r(d)\ [a^{\dagger 2} - a^2]\}$. In order to obtain an output state with the expectations given in Eqs. (11), we should set

$$g_d(\phi_{\rm in}) = 2\frac{\sqrt{1 - 2d\cos(2\phi_{\rm in}) + d^2}}{1 - d^2}, \tag{15a}$$

$$\delta\phi_d(\phi_{\rm in}) = \arctan\left(\frac{1+d}{1-d}\tan\phi_{\rm in}\right) - \phi_{\rm in}, \tag{15b}$$

$$\exp[r(d)] = \frac{1+d}{1-d}. \tag{15c}$$

The block scheme defines a quantum CP-map $\mathcal{E}_{\rm OPO}$ such that $\mathcal{E}_{\rm OPO}(|\alpha e^{i\phi_{\rm in}}\rangle\langle\alpha e^{i\phi_{\rm in}}|) = \rho_{\rm OPO}$ and this approach proves to be equivalent to the input-output one. Moreover, since the block scheme involves the subsequent application of unitary operations associated with linear or bilinear Hamiltionians [32], we conclude that $\rho_{\rm OPO}$ is a Gaussian state and $\mathcal{E}_{\rm OPO}$ is a Gaussian CP-map. Therefore, prime and second moments suffice for a full description of the output state.

4. Case I : phase estimation of a quantum state

Let us now address the case I of Fig. 1. We consider as probe a coherent state $\rho_0 = |\alpha\rangle\langle\alpha|$, $\alpha \in \mathbb{R}_+$, assuming, without loss of generality, the average value of its phase to be fixed. Indeed, it is typically possible to control the average phase by employing a suitable feedback protocol [18, 33]. The coherent seed undergoes phase noise (Fig. 1), whose overall effect is the application of a random phase shift Gaussian-distributed [14, 23, 24]. That is

$$\rho_D = \mathcal{E}_\sigma(|\alpha\rangle\langle\alpha|) = \int_{\mathbb{R}} d\psi\ \frac{e^{-\psi^2/(2\sigma^2)}}{\sqrt{2\pi\sigma^2}}\ U_\psi|\alpha\rangle\langle\alpha|U_\psi^\dagger, \tag{16}$$

where $U_\psi = e^{-i\psi a^\dagger a}$ is a phase shift operation and σ is the amplitude of the noise. Then, following the case I of Fig. 1, we let the dephased state pass through an OPO, described by the map $\mathcal{E}_{\rm OPO}$, obtaining the final state $\rho_{\rm out} = \mathcal{E}_{\rm OPO}\big(\mathcal{E}_\sigma(|\alpha\rangle\langle\alpha|)\big)$. The task is to find a feasible strategy to measure the optical phase and to state whether the OPO is able to compensate the effects of phase noise by comparing the results obtained with states ρ_D and $\rho_{\rm out}$.

Fig. 3 shows the effects of such transformations at the level of quantum states. In the phase space dephasing causes a in-homogeneous spread of the coherent state which makes state ρ_D not Gaussian anymore. Then, the action of the OPO squeezes quadrature p at the expense of magnifying the variance of q.

To give an estimate of the phases of ρ_D and $\rho_{\rm out}$ and assess whether the OPO can *squeeze* the noise, we will consider two different approaches. First of all, we perform a *direct measurement* of the phase, exploiting a phase POVM. Then, we present an *indirect measurement* procedure based on a post processing on the data of two separate homodyne detections, which we will prove to give the same qualitative results in the regime of $\alpha \gg 1$. Actually, given this scenario, we have a priori information that the value of the phase is 0. However, the purpose of both strategies is to choose a proper figure of merit for the phase uncertainty and to state whether or not the OPO is able to reduce such uncertainty.

4.1. Direct measurement of the phase

A convenient way to perform phase estimation is to employ a genuine phase POVM [9, 10, 34]. Among all possible choices, here we consider a feasible POVM, implemented through a heterodyne

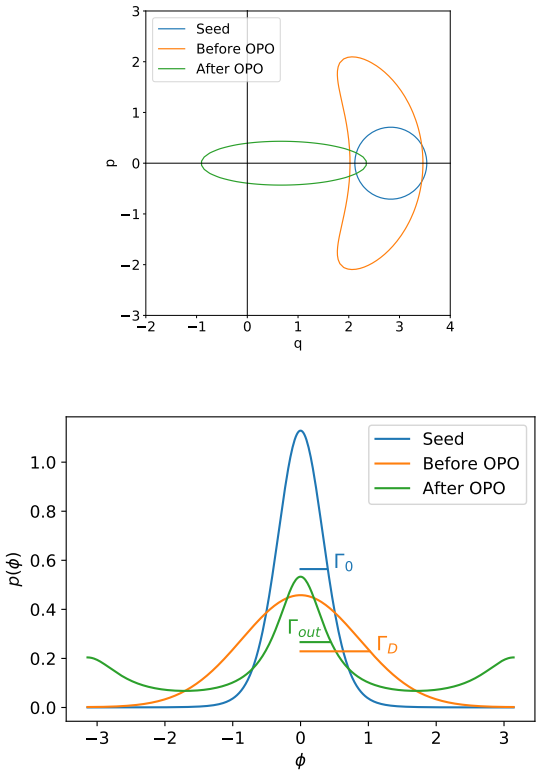

Fig. 3. Top: phase space representation of ρ_0, ρ_D and ρ_{out} where we plot the level curves at the level of the standard deviation. Bottom: phase distributions $p_0(\phi)$, $p_D(\phi)$, $p_{\text{out}}(\phi)$. We set $\alpha = 2$, $\sigma = \pi/4$, $d = 0.4$ and we used the realistic parameters $\eta_{\text{in}} = 0.01$, $\eta_{\text{esc}} = 0.93$.

detection, namely

$$\Pi_\phi = \frac{1}{\pi}\int_0^\infty d\zeta\ \zeta\ |\zeta e^{i\phi}\rangle\langle\zeta e^{i\phi}|, \tag{17}$$

where $|\zeta e^{i\phi}\rangle$ is a coherent state. The corresponding phase probability for a given state ρ reads

$$p(\phi) = \text{Tr}[\rho\Pi_\phi], \tag{18}$$

$$= \int_0^\infty d\zeta\ \zeta\ Q[\rho](\zeta e^{i\phi}), \tag{19}$$

that is the marginal in phase of the Husimi Q-function $Q[\rho](z) = \langle z|\rho|z\rangle/\pi$, $z \in \mathbb{C}$.

Within this scenario, we have to compare the probabilities $p_0(\phi)$, $p_D(\phi)$ and $p_{\text{out}}(\phi)$ associated with the initial state ρ_0, the dephased state ρ_D and the output state ρ_{out}, respectively, and we have to assess in which conditions the OPO leads to a reduction of the width of the distribution. Figure 3 shows the three phase distributions. Compared to the input probability density, dephasing broadens the distribution, while squeezing introduces two secondary peaks at $\pm\pi$: a border effect caused by the π-periodicity of the squeezing phase. Because of this latter effect the proper figure of merit for the phase uncertainty shall be the half width at half maximum (HWHM) of the central peak.

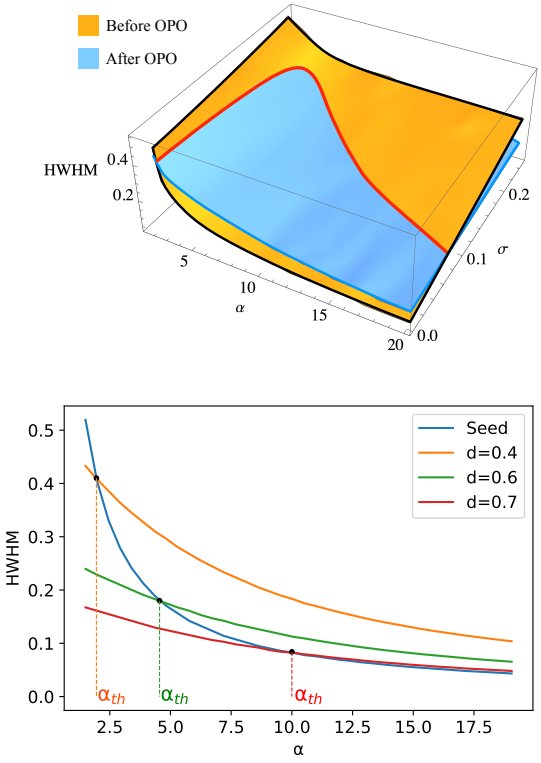

Fig. 4. Top: 3D plot of the dephased HWHM Γ_D and the squeezed HWHM Γ_{out} as function of α and σ, with $d = 0.4$. There exists a threshold signal α_{th} such that for smaller α, $\Gamma_{\text{out}} < \Gamma_D$ for all σ, while for larger α the intersection between the two surfaces identifies the threshold noise σ_{th}. Bottom: plot of the HWHMs Γ_0 of the seed and Γ_S for different values of d as functions of α in the absence of noise ($\sigma = 0$). The intersection between Γ_0 and Γ_S defines the threshold α_{th}, which appears to be an increasing function of d. We used the realistic parameters $\eta_{\text{in}} = 0.01$, $\eta_{\text{esc}} = 0.93$.

Numerical evaluation of $p(\phi)$ in different regimes allows us to understand the role of the different parameters. We fix the OPO parameters $d, \eta_{\text{in}}, \eta_{\text{esc}}$ considering realistic values [23] and consider several values for α and σ. Then, we compute and compare the HWHMs of the dephased distribution $\Gamma_D(\alpha, \sigma)$ and of the squeezed one $\Gamma_{\text{out}}(\alpha, \sigma, d, \eta_{\text{in}}, \eta_{\text{esc}})$. As shown in Fig. 4, if the coherent signal α is small enough, Γ_{out} is constantly inferior than Γ_D, therefore the OPO proves to be always helpful regardless the values of σ. The reason is that even with zero noise, $\sigma = 0$, there exists a regime where the squeezed HWHM $\Gamma_S(\alpha, d, \eta_{\text{in}}, \eta_{\text{esc}}) = \Gamma_{\text{out}}(\alpha, \sigma = 0, d, \eta_{\text{in}}, \eta_{\text{esc}})$ is smaller than the HWHM of the seed probability distribution $\Gamma_0(\alpha)$, since for small α the border peaks of the squeezed distribution centred in $\pm\pi$ induce a non-negligible reduction of the width of the central peak centred in 0. As a consequence, there exists a threshold coherent amplitude $\alpha_{\text{th}}(d, \eta_{\text{in}}, \eta_{\text{esc}})$ such that if $\alpha < \alpha_{\text{th}}(d, \eta_{\text{in}}, \eta_{\text{esc}})$ the OPO is always useful. The threshold is obtained by imposing the equality $\Gamma_0(\alpha_{\text{th}}) = \Gamma_S(\alpha_{\text{th}}, d, \eta_{\text{in}}, \eta_{\text{esc}})$. On the contrary, if $\alpha > \alpha_{\text{th}}(d, \eta_{\text{in}}, \eta_{\text{esc}})$ we observe a σ-dependency. For small noise σ, we have $\Gamma_{\text{out}} > \Gamma_D$ and so the OPO reveals useless, but on the contrary for large noise σ the situation is reversed and $\Gamma_{\text{out}} < \Gamma_D$. There exists a threshold noise $\sigma_{\text{th}}(\alpha, d, \eta_{\text{in}}, \eta_{\text{esc}})$ such that the OPO keeps useful only for $\sigma > \sigma_{\text{th}}(\alpha, d, \eta_{\text{in}}, \eta_{\text{esc}})$. Formally, such threshold noise is obtained by imposing that $\Gamma_D(\alpha, \sigma_{\text{th}}) = \Gamma_{\text{out}}(\alpha, \sigma_{\text{th}}, d, \eta_{\text{in}}, \eta_{\text{esc}})$.

4.2. Indirect measurement of the phase

The second possible phase estimation method involves two different and independent homodyne measurements of q and p to avoid the unavoidable excess noise induced by joint measurements. The value of the phase is obtained by means of the estimator [23]

$$\hat{\varphi} = \arctan \frac{\langle p \rangle}{\langle q \rangle}. \tag{20}$$

The exploitation of average values guarantees that squeezing border effects are absent and we choose the variance of $\hat{\varphi}$ as a good figure of merit. By exploiting the variance propagation law, we have

$$\Delta^2 \varphi = \frac{\langle q \rangle^2 \Delta^2 p + \langle p \rangle^2 \Delta^2 q}{\left(\langle q \rangle^2 + \langle p \rangle^2\right)^2}, \tag{21}$$

The input state ρ_0 is Gaussian with

$$\langle q \rangle_0 = \sqrt{2}\alpha, \quad \langle p \rangle_0 = 0, \quad \Delta^2 q_0 = \Delta^2 p_0 = 1/2, \tag{22}$$

therefore, $\Delta^2 \varphi_0 = 1/4\alpha^2$. For the dephased state ρ_D we have

$$\langle q \rangle_D = e^{-\sigma^2/2}\sqrt{2}\alpha, \quad \langle p \rangle_D = 0, \tag{23}$$

and

$$\Delta^2 q_D = \frac{1}{2} + \alpha^2 \left(1 - e^{-\sigma^2}\right)^2, \quad \Delta^2 p_D = \frac{1}{2} + \alpha^2 \left(1 - e^{-2\sigma^2}\right), \tag{24}$$

leading to

$$\Delta^2 \varphi_D = \frac{e^{\sigma^2}}{4\alpha^2} + \sinh \sigma^2 > \Delta^2 \varphi_0. \tag{25}$$

Finally, the squeezed dephased state ρ_{out} has

$$\langle q \rangle_{\text{out}} = e^{-\sigma^2/2}\sqrt{2}\tilde{\alpha}_q, \quad \langle p \rangle_{\text{out}} = 0, \tag{26}$$

and

$$\Delta^2 q_{\text{out}} = \Sigma_q^2 + \tilde{\alpha}_q^2 \left(1 - e^{-\sigma^2}\right)^2, \quad \Delta^2 p_{\text{out}} = \Sigma_p^2 + \tilde{\alpha}_p^2 \left(1 - e^{-2\sigma^2}\right), \tag{27}$$

thereafter, we obtain

$$\Delta^2 \varphi_{\text{out}} = \frac{e^{\sigma^2}}{2\tilde{\alpha}_q^2}\Sigma_p^2 + \frac{\tilde{\alpha}_p^2}{\tilde{\alpha}_q^2} \sinh \sigma^2. \tag{28}$$

The variance of $\hat{\varphi}$ is given by two contributions, the former is correlated to the signal-to-noise ratio $\Delta^2 p / \langle q \rangle^2$ of the noiseless state ρ_0, the latter is a pure excess noise term. The excess noise term is always reduced after the OPO since $\tilde{\alpha}_p / \tilde{\alpha}_q < 1$. On the contrary, the signal-to-noise term after the OPO turns out to be lower than before only if $\Sigma_p^2 / \tilde{\alpha}_q^2 < 1/2\alpha^2$. This latter condition defines a threshold squeezing d_{th} at fixed values of η_{in} and η_{esc} via the equation

$$f(d_{\text{th}}) \equiv \frac{4\eta_{\text{in}}\eta_{\text{esc}}}{(1 - d_{\text{th}})^2}\left[1 + \frac{d_{\text{th}}}{\eta_{\text{in}}} e^{-2r(d_{\text{th}})}\right] - 1 = 0, \tag{29}$$

and where $r(d)$ is defined in Eq. (15c). If $d > d_{\text{th}}(\eta_{\text{in}}, \eta_{\text{esc}})$ the OPO proves always useful, otherwise if $d < d_{\text{th}}(\eta_{\text{in}}, \eta_{\text{esc}})$, the OPO amplifies the signal-to-noise ratio on quadratures but reduces the excess noise. For small σ it is the signal-to-noise term to dominate, therefore the OPO is useless. When σ is large the situation is reversed. There is a tradeoff between the two

contributions leading to the existence of a threshold noise $\sigma_{\rm th}$ above which squeezing shows a benefit. The threshold condition leads to

$$\sigma_{\rm th}^2 = \frac{1}{2}\ln\left[\frac{2\alpha^2(\tilde{\alpha}_q^2 - \tilde{\alpha}_p^2)}{\tilde{\alpha}_q^2 + 2\alpha^2(\tilde{\alpha}_q^2 - \tilde{\alpha}_p^2 - \Sigma_p^2)}\right], \tag{30}$$

and it agrees, at least qualitatively, to that obtained with a genuine phase measurement in the regime $\alpha \gg 1$ (see Fig. 4). We notice that this agreement also provides a validation for the estimator in Eq. (20), which itself represents a convenient practical choice for experiments [23].

5. Case II : quantum communication protocol

The second scenario in which we discuss the exploitation of an OPO is quantum communication. In particular, we analyze the protocol depicted in Fig. 1, case II, within the framework of quantum estimation theory. We consider as probe the state

$$\rho_{\rm n} = \mathcal{E}_{\rm OPO}\big(\mathcal{E}_\sigma(|\alpha\rangle\langle\alpha|)\big) \tag{31}$$

on which we encode information by means of a phase shift θ through the unitary $U_\theta = e^{-i\theta a^\dagger a}$. After the encoding stage, the quantum state of radiation is sent into a channel until to reach a receiver, who performs measurements. In this case the task is to decide the optimal POVM $\{\Pi_x\}$ to infer the value of θ. Here, we decide to restrict to a subclass of feasible measurements, i.e. *homodyne measurements*. We investigate how the exploitation of the OPO modifies the QFI and the FI of a homodyne detection of $x_\phi = \cos\phi\ q + \sin\phi\ p$. By comparing the two of them, we decide whether homodynes can be optimal and, in particular, which is the best quadrature $x_{\phi_{\rm max}}$ that maximizes the FI. In the following, first of all we analyze the case in absence of phase diffusion as a benchmark and, secondly, we discuss the noisy case.

5.1. Noiseless estimation scheme

In the absence of phase noise (but with the OPO still present), the probe state of the protocol in Fig. 1, case II, is the state $\rho_{\rm OPO}$ derived in sec. 3. Then, the encoded state reads

$$\rho_{{\rm nl},\theta} = U_\theta\ \rho_{\rm OPO}\ U_\theta^\dagger. \tag{32}$$

$\rho_{\rm OPO}$ being a Gaussian state with prime moments $\mathbf{R}_{\rm OPO} \equiv \langle\hat{\mathbf{r}}\rangle = (\sqrt{2}\tilde{\alpha}_q, 0)$ and covariance $\boldsymbol{\sigma}_{\rm OPO} \equiv \langle\{(\hat{\mathbf{r}} - \mathbf{R}_{\rm OPO}), (\hat{\mathbf{r}} - \mathbf{R}_{\rm OPO})^T\}\rangle/2 = {\rm Diag}[\Sigma_q^2, \Sigma_p^2]$, $\hat{\mathbf{r}} = (q, p)$. Therefore, the statistical model $\rho_{{\rm nl},\theta}$ is still Gaussian with prime moments $\mathbf{R}_\theta = \mathcal{R}_\theta\mathbf{R}_{\rm OPO}$ and covariance $\boldsymbol{\sigma}_\theta = \mathcal{R}_\theta\boldsymbol{\sigma}_{\rm OPO}\mathcal{R}_\theta^T$, where $\mathcal{R}_\theta$ is the rotation matrix

$$\mathcal{R}_\theta = \begin{pmatrix} \cos\theta & \sin\theta \\ -\sin\theta & \cos\theta \end{pmatrix}. \tag{33}$$

In general, for a generic Gaussian state ρ_λ with prime moments $\mathbf{R}_\lambda$ and covariance $\boldsymbol{\sigma}_\lambda$, the QFI has the following analytical expression,

$$H(\lambda) = \frac{1}{2}\frac{{\rm Tr}\big[(\boldsymbol{\sigma}_\lambda^{-1}\boldsymbol{\sigma}_\lambda')^2\big]}{1+\mu_\lambda^2} + 2\frac{\mu_\lambda'^2}{1-\mu_\lambda^4} + \mathbf{R}_\lambda'^T\boldsymbol{\sigma}_\lambda^{-1}\mathbf{R}_\lambda', \tag{34}$$

where the $A' = \partial_\lambda A$ and $\mu_\lambda = (2\sqrt{\det\boldsymbol{\sigma}_\lambda})^{-1}$ is the purity of the Gaussian state ρ_λ [35–38].

In the very case in exam, Eq. (34) leads to

$$H_{\rm nl} = 4\frac{(\Sigma_q^2 - \Sigma_p^2)^2}{1 + 4\Sigma_p^2\Sigma_q^2} + 2\frac{\tilde{\alpha}_q^2}{\Sigma_p^2}, \tag{35}$$

which is independent of θ. The QFI depends on both α and d. However, the α-dependence is only polynomial and so less relevant than the squeezing one. Therefore, in the following we keep α fixed and study the QFI dependence on the squeezing factor $r = \ln[(1+d)/(1-d)]$. As depicted in Fig. 6, the QFI is a growing function on r. Thus, the most sensitive probe is obtained for $r \gg 1$, i.e. $d \approx 1$. It is also worth to find out the asymptotic scaling of the QFI, by evaluating its dependence on the energy

$$N = \mathrm{Tr}[\rho_{\mathrm{nl},\theta} a^\dagger a] = \frac{\Sigma_q^2 + \Sigma_p^2 + \tilde{\alpha}_q^2 - 1}{2}, \tag{36}$$

by keeping α fixed and varying only d. Eventually, the QFI H_{nl} shows shot noise scaling:

$$H_{\mathrm{nl}} \approx \frac{4}{1-\eta_{\mathrm{esc}}} \frac{1+4\eta_{\mathrm{in}}\alpha^2}{1+2\eta_{\mathrm{in}}\alpha^2} N, \tag{37}$$

whose origin can be addressed to the non-negligible losses characterizing the OPO dynamics.

As regards the FI analysis, it is helpful to write the probe state ρ_{OPO} in the form of a displayed squeezed thermal state [32, 39]

$$\rho_{\mathrm{OPO}} = D(\beta)\, S(\xi)\, \nu^{\mathrm{th}}(\bar{n})\, S(\xi)^\dagger\, D(\beta)^\dagger, \tag{38}$$

where $D(\beta) = \exp(\beta a^\dagger - \beta^* a)$ is the displacement operator, $S(\xi) = \exp[\frac{1}{2}\xi(a^{\dagger 2} - a^2)]$ is the squeezing operator and $\nu^{\mathrm{th}}(\bar{n}) = \bar{n}^{a^\dagger a}/(\bar{n}+1)^{a^\dagger a+1}$ is a thermal state with mean number of photons $\bar{n}$. For the state ρ_{OPO} the values of the parameters are $\beta = \tilde{\alpha}_q$, $\exp(2\xi) = \sqrt{\Sigma_q^2/\Sigma_p^2}$, $(1+2\bar{n})^2 = 4\Sigma_q^2\Sigma_p^2$.

Actually, it is proved that for a displayed squeezed thermal state the optimal measurement is not Gaussian [40] and no homodyne can exactly reach the QFI. Nevertheless, it is still worth to construct an optimized homodyne measurement since it becomes nearly optimal (i.e. FI $\approx$ QFI) in the best working regime $r \gg 1$.

To construct the optimized homodyne, we keep again α fixed and let only the squeezing parameter r vary. For every r, we compute the FI associated with $x_\phi = \cos\phi\ q + \sin\phi\ p$ as a function of ϕ and find the value ϕ_{max} maximizing it, as depicted in Fig. 5. In the end, the optimized FI F_{nl} turns out to be a piecewise-defined function, since there exist two quadratures candidated to the choice of ϕ_{max} [40]:

1. $\phi^{(1)} = \pi/2 - \theta$ whose corresponding FI is

$$F^{(1)} = \frac{2\tilde{\alpha}_q^2}{\Sigma_p^2}, \tag{39}$$

2. $\phi^{(2)} = \pi/2 - \theta - \chi/2$, where χ satisfies

$$\cos\chi = \frac{(\Sigma_q^2 - \Sigma_p^2)^3 + \Sigma_q^2\tilde{\alpha}_q^2(\Sigma_q^2 + \Sigma_p^2)}{(\Sigma_q^2 + \Sigma_p^2)(\Sigma_q^2 - \Sigma_p^2)^2 + \Sigma_q^2\tilde{\alpha}_q^2(\Sigma_q^2 - \Sigma_p^2)} \quad (d \neq 0), \tag{40}$$

for which the corresponding value of the FI reads

$$F^{(2)} = \frac{\left[(\Sigma_q^2 - \Sigma_p^2)^2 + \Sigma_q^2\tilde{\alpha}_q^2\right]^2}{2\Sigma_q^2\Sigma_p^2(\Sigma_q^2 - \Sigma_p^2)^2}. \tag{41}$$

The second measurement is well defined only if $|\cos\chi| \leq 1$, that is

$$\tilde{\alpha}_q \leq (\Sigma_q^2 - \Sigma_p^2)/\sqrt{\Sigma_q^2}, \tag{42}$$

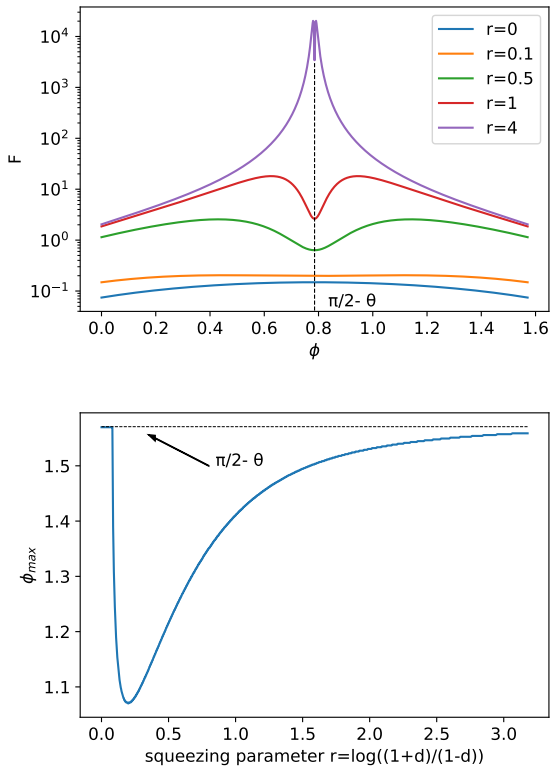

Fig. 5. Top: FI of the measurement of x_ϕ as a function of ϕ for different values of the squeezing parameter r. Bottom: optimized quadrature $\phi_{\max}$ as a function of r. We set $\alpha = 1$ and we used the realistic parameters $\eta_{\rm in} = 0.01$, $\eta_{\rm esc} = 0.93$.

providing a threshold squeezing $r_{\rm th}(\alpha, \eta_{\rm in}, \eta_{\rm esc})$ such that for smaller r the optimized quadrature is $\phi^{(1)}$, while for larger r the optimized quadrature becomes $\phi^{(2)}$. The physical explanation of such behaviour becomes clear by observing the ϕ dependence of the FI displayed in Fig. 5. For small r, the function has a single maximum at $\pi/2 - \theta$, but for larger r the maximum splits into two symmetric peakes and $\pi/2 - \theta$ turns into a local minimum. Then, by increasing r further the position of the peakes asymptotically converges to $\pi/2 - \theta$. As regards the energy scaling of $F_{\rm nl}$, by rearranging Eq. (41) we get again shot noise scaling

$$F_{\rm nl} \approx 2\frac{1 + 2\eta_{in}\alpha^2}{1 - \eta_{esc}}\, N. \tag{43}$$

5.2. *Noisy estimation scheme*

If phase noise is present, the statistical model reads

$$\rho_{{\rm n},\theta} = U_\theta\, \rho_{\rm n}\, U_\theta^\dagger, \tag{44}$$

where $\rho_{\rm n}$ is still given in Eq. (31). The presence of the this kind of noise prevents to obtain analytical solutions. Therefore, we keep the results of sec. 5.1 as a benchmark and consider how the noise affects a specific case. We perform a homodyne of $x_{\phi_{\max}}$, where $\phi_{\max}$ is the optimized

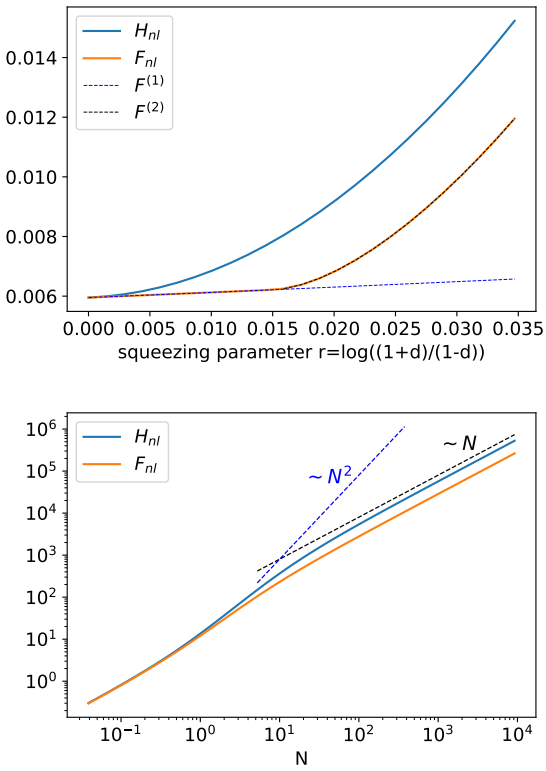

Fig. 6. Top: QFI and optimized FI as a function of r. Bottom: QFI and optimized FI as a function of N (plot in log scale). The dashed lines refer to the Heisenberg scaling $\sim N^2$ and shot-noise one $\sim N$. We set $\alpha = 0.2$ and we used the realistic parameters $\eta_{\rm in} = 0.01$, $\eta_{\rm esc} = 0.93$.

quadrature of Fig. 5. For several values of σ, we analyze the dependence of the FI

$$F_{\rm n} = \int dx \frac{\left[\partial_\theta p(x|\theta)\right]^2}{p(x|\theta)}, \qquad p(x|\theta) = {\rm Tr}[\rho_{{\rm n},\theta}\, x_{\phi_{\rm max}}], \tag{45}$$

on the energy N of Eq. (36). Moreover, to compare the noiseless and noisy cases we introduce the relative fluctuations parameter

$$\epsilon = \frac{|F_{\rm n} - F_{\rm nl}|}{F_{\rm nl}}. \tag{46}$$

The numerical results of ϵ, depicted in Fig. 7, show that the exploitation of the OPO is able to compensate almost completely the detriments of phase noise. In particular, using an OPO is crucial to maintain the shot noise regime for all values of σ. Otherwise, if we consider the protocol of Fig. 1, case II, without the OPO, there exists an upper bound for the QFI [41], namely

$$H_{\text{without OPO}} \leq H_{\rm UB} = \frac{4N}{1 + 4N\sigma^2}, \tag{47}$$

saturating for large N to the value $1/\sigma^2$.

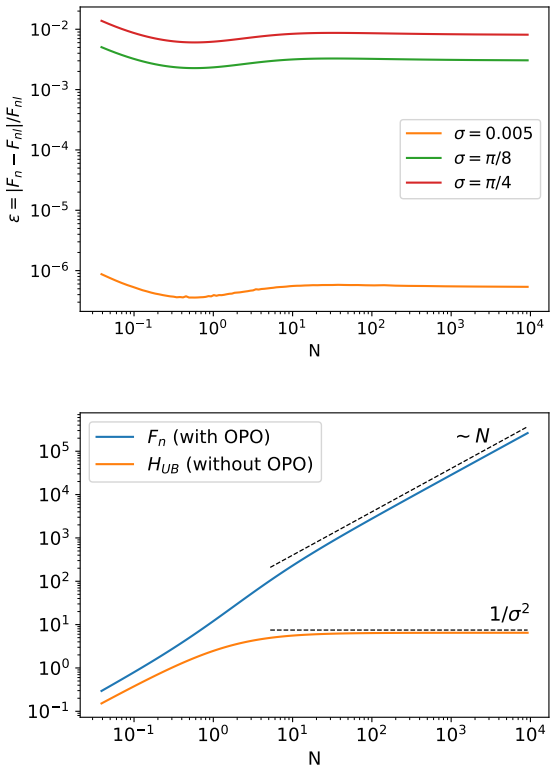

Fig. 7. Top: Relative fluctuations ϵ given in Eq. (46) as a funtcion of N for different values of the noise parameter σ. Bottom: Plot of the $F_{\rm n}$ and $H_{\rm UB}$ as functions of N for $\sigma = \pi/8$. We set $\theta = 0$, $\alpha = 0.2$ and we used the realistic parameters $\eta_{\rm in} = 0.01$, $\eta_{\rm esc} = 0.93$.

6. Conclusions

In summary, we have studied several scenarios where phase noise prevents the use of optical phase as a degree of freedom for quantum information tasks and discussed whether an OPO may be employed to mitigate, or even compensate, the effects of noise.

At first, we have developed a block-diagram model to describe an OPO in the form of a subsequent application of Gaussian operations: beam splitters, phase-sensitive amplification, phase-sensitive phase shift and squeezing. Such description in the Schrödinger picture allows to give an explicit expression for the output state of radiation. Indeed, given a initial coherent state the output state is a Gaussian state with well-defined prime moments and covariance.

With the new description of the OPO we have addressed the first scenario under investigation: a measurement of the phase of a quantum state of radiation. We have introduced two possible approaches. A first standard approach involves the introduction of a phase POVM (implemented through heterodyne detection). It leads to the conclusion that the OPO reduces phase noise, i.e. the width of the probability distribution associated with the POVM, for small signal amplitude, or large signal amplitude and large dephasing. The second approach consists in a post-processing estimation based on the outcomes of two distinct homodyne detections and brings the same phenomenology as before in the regime of large coherent amplitudes. In both cases, according to the value of parameters α, σ, d, there exists a regime where the procedure gives a phase outcome

with a larger uncertainty than the one of the initial coherent state and another regime in which the uncertainty is smaller. This leads to the conclusion that in such regime the OPO is able to *fully*, or at least *partially*, compensate the noise.

The second scenario discussed has been a communication protocol based on the encoding of a phase shift θ on the probe state. We have considered a dephased coherent state passed through an OPO as probe state and searched for the optimal POVM to detect θ within the subclass of homodyne measurements. We have studied in detail the noiseless protocol, obtaining the optimized quadrature $\phi_{\max}$ that allows to infer θ with negligible uncertainty. Passing to the noisy case, such situation is still maintained. The noise affects weakly the FI and shot noise scaling, i. e. the proper scaling of the input coherent state, is conserved. Therefore, in such case the noise mitigation by the OPO is *complete* as regards the scaling with the probe average photon number.

Our results confirm that it is possible to develop suitable OPO-based strategies to compensate phase noise with current technology and, thus, pave the way for the full exploitation of optical phase in quantum technologies.

Acknowledgements

This work has been supported by MAECI, Project No. PGR06314 "ENYGMA" and by University of Milan, Project No. RV-PSR-SOE-2020-SOLIV "S-O PhoQuLis"

References

1. C. M. Caves, "Quantum-mechanical noise in an interferometer," Phys. Rev. D **23**, 1693–1708 (1981).
2. R. Demkowicz-Dobrzański, U. Dorner, B. J. Smith, J. S. Lundeen, W. Wasilewski, K. Banaszek, and I. A. Walmsley, "Quantum phase estimation with lossy interferometers," Phys. Rev. A **80**, 013825 (2009).
3. C. Sparaciari, S. Olivares, and M. G. A. Paris, "Bounds to precision for quantum interferometry with Gaussian states and operations," J. Opt. Soc. Am. B **32**, 1354–1359 (2015).
4. L. G. Kazovsky, G. Kalogerakis, and W. Shaw, "Homodyne phase-shift-keying systems: Past challenges and future opportunities," J. Light. Technol. **24**, 4876–4884 (2006).
5. S. Olivares, S. Cialdi, F. Castelli, and M. G. A. Paris, "Homodyne detection as a near-optimum receiver for phase-shift-keyed binary communication in the presence of phase diffusion," Phys. Rev. A **87**, 050303 (2013).
6. M. Mondin, F. Daneshgaran, I. Bari, M. T. Delgado, S. Olivares, and M. G. A. Paris, "Soft-metric-based channel decoding for photon counting receivers," IEEE J. Sel. Top. Quantum Electron. **21**, 62–68 (2015).
7. L. Susskind and J. Glogower, "Quantum mechanical phase and time operator," Phys. Physique Fizika **1**, 49 (1964).
8. W. H. Louisell, "Amplitude and phase uncertainty relations," Phys. Lett. **7**, 60–61 (1963).
9. G. M. D'Ariano and M. G. A. Paris, "Lower bounds on phase sensitivity in ideal and feasible measurements," Phys. Rev. A **49**, 3022–3036 (1994).
10. D. I. Lalović, D. M. Davidović, and A. R. Tančić, "Quantum phase from the glauber model of linear phase amplifiers," Phys. Rev. Lett. **81**, 1223–1226 (1998).
11. E. Ip, A. P. T. Lau, D. J. F. Barros, and J. M. Kahn, "Coherent detection in optical fiber systems," Opt. Express **16**, 753–791 (2008).
12. D. Brivio, S. Cialdi, S. Vezzoli, B. T. Gebrehiwot, M. G. Genoni, S. Olivares, and M. G. A. Paris, "Experimental estimation of one-parameter qubit gates in the presence of phase diffusion," Phys. Rev. A **81**, 012305 (2010).
13. B. Teklu, M. G. Genoni, S. Olivares, and M. G. A. Paris, "Phase estimation in the presence of phase diffusion: the qubit case," Phys. Scripta **2010**, 014062 (2010).
14. M. G. Genoni, S. Olivares, and M. G. A. Paris, "Optical phase estimation in the presence of phase diffusion," Phys. Rev. Lett. **106**, 153603 (2011).
15. M. G. Genoni, S. Olivares, D. Brivio, S. Cialdi, D. Cipriani, A. Santamato, S. Vezzoli, and M. G. A. Paris, "Optical interferometry in the presence of large phase diffusion," Phys. Rev. A **85**, 043817 (2012).
16. J. Trapani, B. Teklu, S. Olivares, and M. G. A. Paris, "Quantum phase communication channels in the presence of static and dynamical phase diffusion," Phys. Rev. A **92**, 012317 (2015).
17. M. Jarzyna, V. Lipińska, A. Klimek, K. Banaszek, and M. G. A. Paris, "Phase noise in collective binary phase shift keying with hadamard words," Opt. Express **24**, 1693–1698 (2016).
18. M. Bina, A. Allevi, M. Bondani, and S. Olivares, "Phase-reference monitoring in coherent-state discrimination assisted by a photon-number resolving detector," Sci. Reports **6**, 1–9 (2016).
19. M. T. DiMario, L. Kunz, K. Banaszek, and F. E. Becerra, "Optimized communication strategies with binary coherent states over phase noise channels," npj Quantum Inf. **5**, 65 (2019).
20. I. Tikhonenkov, M. G. Moore, and A. Vardi, "Optimal Gaussian squeezed states for atom interferometry in the presence of phase diffusion," Phys. Rev. A **82**, 043624 (2010).

21. Y. C. Liu, G. R. Jin, and L. You, "Quantum-limited metrology in the presence of collisional dephasing," Phys. Rev. A **82**, 045601 (2010).
22. G. Ferrini, D. Spehner, A. Minguzzi, and F. W. J. Hekking, "Noise in Bose Josephson junctions: Decoherence and phase relaxation," Phys. Rev. A **82**, 033621 (2010).
23. S. Cialdi, E. Suerra, S. Olivares, S. Capra, and M. G. A. Paris, "Squeezing phase diffusion," Phys. Rev. Lett. **124**, 163601 (2020).
24. G. Carrara, M. G. Genoni, S. Cialdi, M. G. A. Paris, and S. Olivares, "Squeezing as a resource to counteract phase diffusion in optical phase estimation," Phys. Rev. A **102**, 062610 (2020).
25. M. G. A. Paris, "Quantum estimation for quantum technology," Int. J. Quantum Inf. **7**, 125–137 (2009).
26. C. W. Helstrom, *Quantum Detection and Estimation Theory*, Mathematics in Science and Engineering 123 (Elsevier, Academic Press, 1976).
27. J. D. Malley and J. Hornstein, "Quantum statistical inference," Stat. Sci. pp. 433–457 (1993).
28. S. L. Braunstein and C. M. Caves, "Statistical distance and the geometry of quantum states," Phys. Rev. Lett. **72**, 3439 (1994).
29. S. L. Braunstein, C. M. Caves, and G. J. Milburn, "Generalized uncertainty relations: theory, examples, and lorentz invariance," Annals Phys. **247**, 135–173 (1996).
30. D. C. Brody and L. P. Hughston, "Statistical geometry in quantum mechanics," Proc. Royal Soc. London. Ser. A: Math. Phys. Eng. Sci. **454**, 2445–2475 (1998).
31. H.-A. Bachor and T. C. Ralph, *A Guide to Experiments in Quantum Optics*, Physics textbook (Wiley-VCH, 2004).
32. S. Olivares, "Quantum optics in the phase space," The Eur. Phys. J. Special Top. **203**, 3–24 (2012).
33. G. M. D'Ariano, M. G. A. Paris, and R. Seno, "Feedback-assisted homodyne detection of phase shifts," Phys. Rev. A **54**, 4495–4504 (1996).
34. J. W. Noh, A. Fougères, and L. Mandel, "Measurement of the quantum phase by photon counting," Phys. Rev. Lett. **67**, 1426–1429 (1991).
35. A. Serafini, *Quantum Continuous Variables: A Primer of Theoretical Methods* (CRC Press, Taylor & Francis Group, 2017).
36. O. Pinel, P. Jian, N. Treps, C. Fabre, and D. Braun, "Quantum parameter estimation using general single-mode Gaussian states," Phys. Rev. A **88**, 040102 (2013).
37. A. Monras, "Phase space formalism for quantum estimation of Gaussian states," eprint arXiv:1303.3682 (2013).
38. Z. Jiang, "Quantum fisher information for states in exponential form," Phys. Rev. A **89**, 032128 (2014).
39. A. Ferraro, S. Olivares, and M. G. A. Paris, *Gaussian states in quantum information* (Bibliopolis Napoli, 2005).
40. C. Oh, C. Lee, C. Rockstuhl, H. Jeong, J. Kim, H. Nha, and S.-Y. Lee, "Optimal Gaussian measurements for phase estimation in single-mode gaussian metrology," npj Quantum Inf. **5**, 10 (2019).
41. B. M. Escher, L. Davidovich, N. Zagury, and R. L. de Matos Filho, "Quantum metrological limits via a variational approach," Phys. Rev. Lett. **109**, 190404 (2012).